On the existence of a critical speed of a rotating ring under a stationary point load

Tao Lu Andrei V. Metrikine
T.Lu-2@tudelft.nl

Abstract

It is known that critical speeds exist for a constant load uniformly moving around an elastic ring, which is elastically connected to an immovable axis. However, in the inverted case, namely in the case of a rotating ring subject to a stationary constant load, the existence of such critical speeds is still being debated by the research community. Various rotating thin ring/shell models are available in literature. Especially active is the tire research community within which the rotating ring/shell models are often employed to mimic vibrations of the tire tread of pneumatic tires. The theoretical predictions of the critical speeds made on the basis of the existing models are not convincing and sometimes confusing. Properly formulated governing equations including the pretension due to rotation and a due linearization are needed to predict the critical speeds correctly. In this paper, a rotating thin ring elastically mounted on an immovable axis and subjected to a stationary point load is investigated. The governing equations are obtained by modifying one of the most widely used rotating ring models in order to describe the pretension in a more accurate way. The parameters are adopted from a pneumatic tire. Free and forced vibrations are investigated. Instability and stationary modes are found which were not reported in literature before. The results of the forced vibration clearly reveal that a critical speed of a rotating ring does exist. The deformation patters of the ring rotating at the sub-critical and super-critical speeds are shown and discussed.

1 Introduction

The in-plane vibration of rotating thin rings and shells has wide engineering applications. A special position among those is occupied by the pneumatic tires, whose dynamics has been investigated by many researchers with the help of rotating ring models. Such simplistic models are useful because the predicted natural frequencies are in good agreement with the ones measured in experiments. Various rotating thin ring models have been developed and, among those, the models based on the Loves thin shell theory in Ref. [1, 2, 3] are most commonly used. Critical speed clearly exists for a constant load moving around an elastic ring [4] but the existence of the critical speed for a rotating ring subjected to a stationary constant load is still being debated. Significant wave-like deformation was observed when a pneumatic tire rolls on the ground with a speed higher than a certain critical value which

suggests a rotating ring may have a critical rotation speed. However, the theoretical predictions for the critical speed are not convincing and, sometimes, confusing when use is made of the existing rotating ring models. Some references gave a prediction for the critical speed but the pretension due to rotation was not properly included or even not included at all, e.g. Ref. [5, 6]. Many other references did not mention the critical speed problem, e.g. in [2, 3]. In Ref. [7], Huang and Hsu concluded that no critical rotational speeds exist for the forced response to a stationary constant point load subjected to a rotating thin shell.

The aim of this paper is to show that there exist critical speeds for rotating thin rings but a modification of the model is needed to predict those. The rotating thin ring model used in this paper is a modified version of that presented in ref. [2].The modification concerns the pretension caused by rotation. Parameters from a pneumatic tire are applied. The physical parameters of the ring are obtained by matching the natural frequencies predicted by the adopted analytical model with the measured ones from ref. [8]. Free vibrations are studied first in order to show the effect of the gyroscopic forces. Thereafter, the ring response to a constant stationary point load is analyzed.

2 Governing Equations

In this paper, pneumatic tires are chosen as the engineering application of rotating ring model. The tire is modeled as a thin ring with a uniform rectangular cross section. Radial and circumferential distributed springs are used to model the sidewall of the tire. It is assumed that the center of the ring is fixed and the ring rotates about it.

The rotating ring model and the reference systems are shown in Figure 1. It is assumed that the mean radius of the ring is R, whereas w and u are the small displacements in the radial and circumferential directions, respectively. p is the internal air pressure of the tire. The stiffnesses of the radial and circumferential springs per unit length are designated as k_r and k_c, respectively. It is also assumed that all springs possess viscosity per unit length equal to σ. Furthermore, ρ is the mass density of the rim, E is the Youngs modulus, A is the cross-sectional area and I is the cross sectional moment of inertia. P is the magnitude of the constant radial point load which represents the contact force between the tire and the ground. Ω is the angular frequency of the tire rotation.

The linearized equations governing the model vibrations in the nonrotating reference system are the same as in ref. [2] and can be written as

$$\begin{aligned}
\rho A\ddot{u} + 2\rho A\Omega(\dot{u}' + \dot{w}) - \rho A\Omega^2(u - 2w' - u'') + k_c u + \frac{EI}{R^4}(w''' - u'') - \\
\frac{EA}{R^2}(w' + u'') + N(u - w') + \frac{pb}{R}(w' - u) + \sigma(\dot{u} + \Omega u') = 0, \\
\rho A\ddot{w} + 2\rho A\Omega(\dot{w}' - \dot{u}) - \rho A\Omega^2(w + 2u' - w'') + k_r w + \frac{EI}{R^4}(w'''' - u''') + \\
\frac{EA}{R^2}(w + u') + N(u' - w'') - \frac{pb}{R}(w + u') + \sigma(\dot{w} + \Omega w') = P\delta(\theta),
\end{aligned} \tag{1}$$

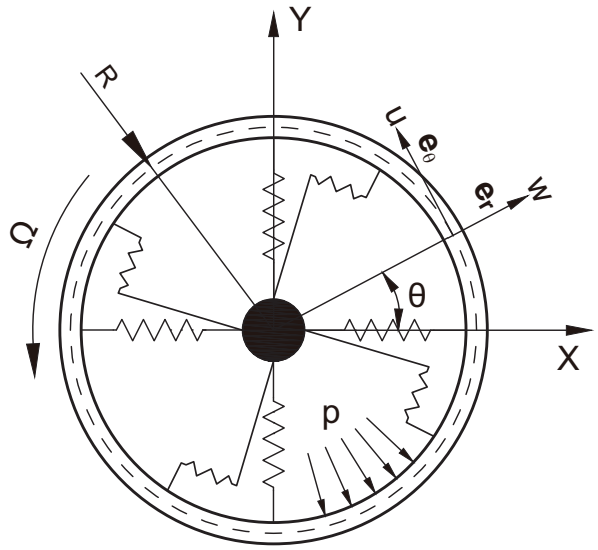

Figure 1: Rotating ring

where the overdot and the prime designate the partial derivatives with respect to time and the angle θ, respectively.

Note that because of rotation, the ring has a static radial deformation w_e and the pretension $N = EAw_e/R$ (see Ref. [2]). Equation (1) governs small vibrations about the static equilibrium.

In Ref. [1, 2, 3] and in most of the other references, the pretension is approximated by

$$N = pbR + \rho AR^2\Omega^2. \tag{2}$$

A proper approximation for the pretension due to rotation is needed to predict the critical speed. If we take an element of the rotating ring and analyze the force equilibrium, the pretension can be shown to be described by

$$N = \frac{EA}{R}\frac{pbR + \rho AR^2\Omega^2}{EA/R + k_r R}. \tag{3}$$

If $EA/R >> k_r R$, i.e. if the extensional stiffness EA of the tire treadband is very high, then the approximation $N = pbR + \rho AR^2\Omega^2$ can be applied. However, in the present paper, the more general equation (3) is retained. Consequently, the static radial deformation is taken as

$$w_e = \frac{pbR + \rho AR^2\Omega^2}{EA/R + k_r R}. \tag{4}$$

3 Identification of the parameters

One of the main factors the validity of the rotating thin ring model depends upon is the estimation of the values for the parameters in the governing equations. A

reasonable way to determine those is to match the natural frequencies predicted by the analytical model with those measured using nonrotating tires [2, 8].

Let us derive expressions for the natural frequencies. To this end, we assume the following form of the solution:

$$w(\theta,t) = We^{i(n\theta+\omega_n t)},\ \ u(\theta,t) = Ue^{i(n\theta+\omega_n t)}. \tag{5}$$

Substituting the above expressions into the governing equation (1), one can obtain the frequency equation in the form of a fourth order polynomial:

$$\omega_n{}^4 + a_3\omega_n{}^3 + a_2\omega_n{}^2 + a_1\omega_n + a_0 = 0. \tag{6}$$

For brevity, the expressions for the coefficients of the above polynomial are omitted. These coefficients are functions of all the model parameters, as well as of the mode number n and speed of rotation Ω.

Generally, the geometrical and material parameters ρ,A,R,b,h(b is the width and h the thickness of the ring), are obtained based on the tire geometry and its material properties. In contrast, the equivalent parameters EA,EI,k_r,k_c are identified from experimental modal analysis. By comparing the measured natural frequencies and natural frequencies predicted by equation (5), the values of EA,EI,k_r,k_c can be identified. The experimental natural frequencies, along with geometrical and material parameters used in this paper are taken from Ref. [8] for a 195/70R14 radial tire. The geometrical and material parameters are

$$b = 0.16m,\ h = 0.01m,\ A = 0.0016m^2,\ R = 0.285m,$$
$$\rho = 2.28\times10^3 kg/m^3,\ p = 2.5\times10^5 N/m^2$$

Table 1: The measured and theoretically predicted natural frequencies

	Mode number	n=1	n=2	n=3	n=4	n=5	n=6	n=7	n=8
1	f_n(Hz):measured	-	108.53	132.38	158.30	186.92	213.60	248.14	287.54
2	f_n(Hz):predicted	91.14	108.53	132.38	159.32	186.92	215.17	245.92	287.54

The first row in Table 1 lists the measured natural frequencies of the tire adopted from Ref. [8]. The second row contains the natural frequencies predicted by the model whose parameters were chosen such as to give a close correspondence between the measured and calculated frequencies. In order to determine four equivalent parameters, namely EA,EI,k_r,k_c four measured natural frequencies were substituted in the characteristic equation (6).

The natural frequencies of n=2, 3, 5, 8 were used. Upon solving the four obtained nonlinear algebraic equations the following figures for the equivalent parameters were obtained:

$$EA = 13374.99N,\ EI = 17.37Nm^2,\ k_r = 4.49\times10^6 N/m^2,\ k_c = 1.16\times10^6 N/m^2$$

Substituting the above figures to equation (6) and solving it for the frequency, the natural frequencies shown in the last row of Table 1 were obtained. Table 1 demonstrates good agreement between the theoretical and measured natural frequencies. Note that in Table 1, the measured natural frequencies are associated with the dominant bending modes. Since no inextensibility assumption is employed here, the natural frequencies of the extensional modes can be obtained as well by solving equation (6).

4 Free vibration

Making use of the identified equivalent parameters, the natural frequencies of the rotating ring can be obtained. The dependence of the natural frequencies on the rotation speed for the modes from 0 to 5 are shown in Figure 2. The absolute values of the real part of the natural frequencies are shown.

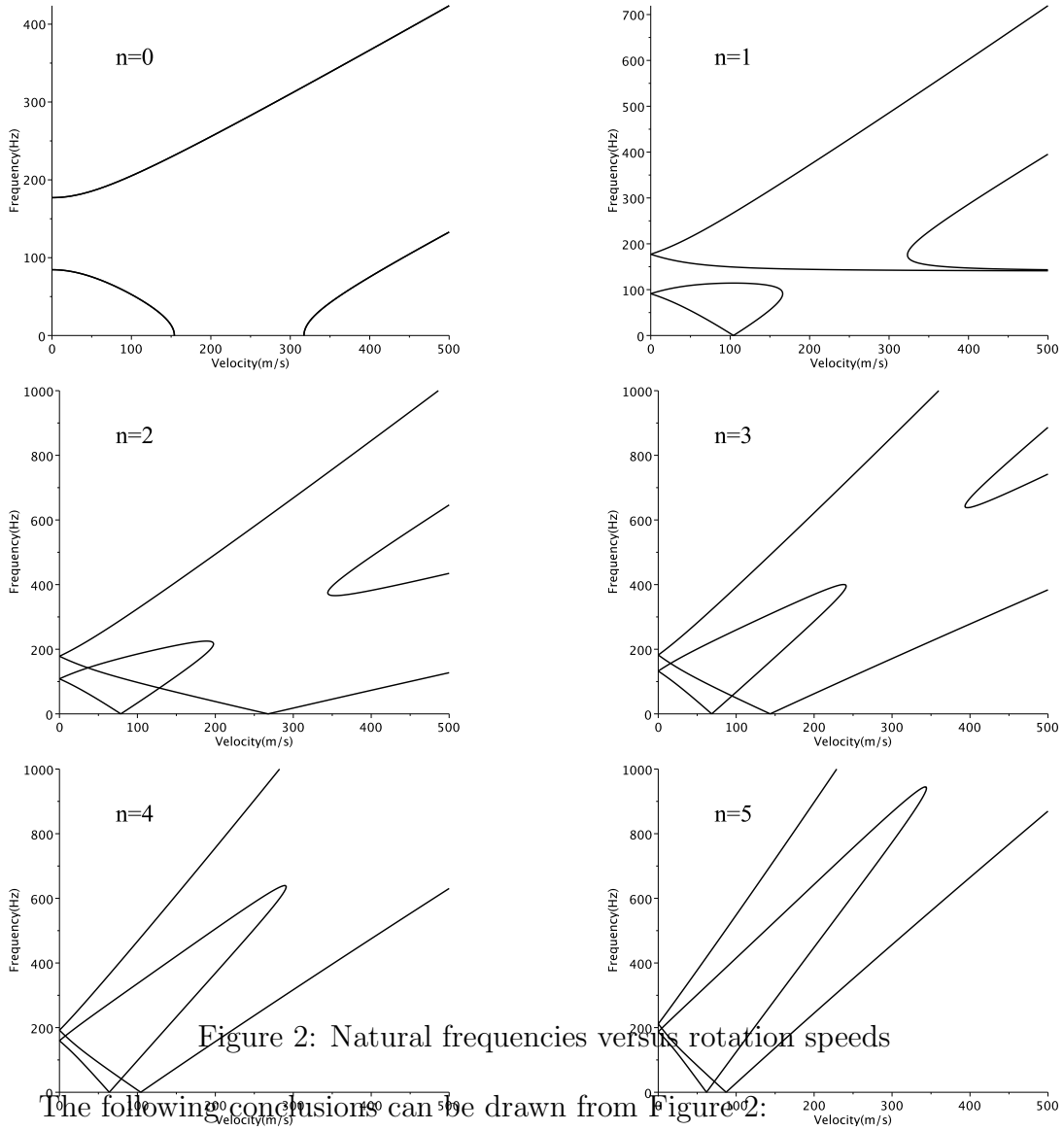

Figure 2: Natural frequencies versus rotation speeds

The following conclusions can be drawn from Figure 2:

1. Frequency bifurcation. The nonrotating ring has two distinct natural frequencies (for each mode number) associated predominantly with the radial and circumferential vibrations. Usually, the lower one corresponds to the predominantly radial motion while the higher one is associated with the predominantly circumferential motion(for $n \geq 2$). When the ring rotates, for any mode number greater than zero, both the lower and the higher natural frequencies split into two different frequen-

cies which results in four distinct natural frequencies. This phenomenon is referred to as the frequency bifurcation. One needs to note that the natural frequencies corresponding to n=0 do not bifurcate.

2. Instability. For mode 0, the higher natural frequency increases monotonically as the rotation speed grows, whereas the lower one first decreases to zero and then its real part turns to zero at certain velocity. This means that as from this velocity (and up to the velocity at which the real part becomes nonzero again) the natural frequency is purely imaginary which indicates that the system is unstable and the type of the instability is divergence. For the modes $n \geq 1$, the two distinct natural frequencies of the lower set coalesce into one at a particular velocity and become complex-valued after this velocity. When the speed of rotation increases further, the natural frequencies may become real again. Since the coefficients of the characteristic polynomial (6) are all real, the complex roots appear in conjugate pairs. Therefore, there must be at least one root with negative imaginary part. This means the motion in unstable and flutter instability may occur.

3. Stationary modes. For the modes $n \geq 1$, zero natural frequencies are observed at certain speeds of rotation for both predominantly radial and predominantly circumferential vibrations. In the case of zero frequency, equation (5) reduces to

$$w(\theta, t) = We^{in\theta}, \;\; u(\theta, t) = Ue^{in\theta} \tag{7}$$

and the deformation of the ring becomes time independent. This means that the modes corresponding to zero natural frequencies are stationary with respect to an earth-bound observer. This phenomenon was not reported in literature.

4. The natural frequencies of both the radial and circumferential modes are nearly the same in the case of a nonrotating tire ($\Omega = 0$). This fact has been confirmed by many modal tests in literature, for example in Ref. [9].

The maximum velocity in Figure 2 is 500m/s. The operational speed of a tire cannot reach such high a velocity in reality. Furthermore, even if it would, the validity of the model would be jeopardized by a very large static deformation. Therefore, the predictions of the natural frequencies for the high rotation speeds are provided herein for the sake of the completeness of the mathematical analysis only.

5 Steady-state response of a rotating ring

In this section, the forced vibration of a rotating ring is computed. The so-called method of images is employed to solve the governing equations. This method was first used to solve the response of an elastic ring subject to a moving load in Ref. [4] and recently applied for computing the response of a rotating train wheel in [10]. The parameters have been given in Section 3.

Figures 3-5 show the radial displacement w, the circumferential displacement u and the corresponding ring shapes for three different rotating speeds. The magnitude of the applied force is 1.0×10^4N and the damping σ used is 500Ns/m^2. In figures 3-5(a), the radial and circumferential displacements are plotted versus the distance from the load ξ ($\xi = 0$ is the loading point,$\xi > 0$ corresponds to the position when $0 < \theta \leq \pi$, $\xi < 0$ corresponds to the position when $\pi < \theta \leq 2\pi$). In figures 3-5(b),

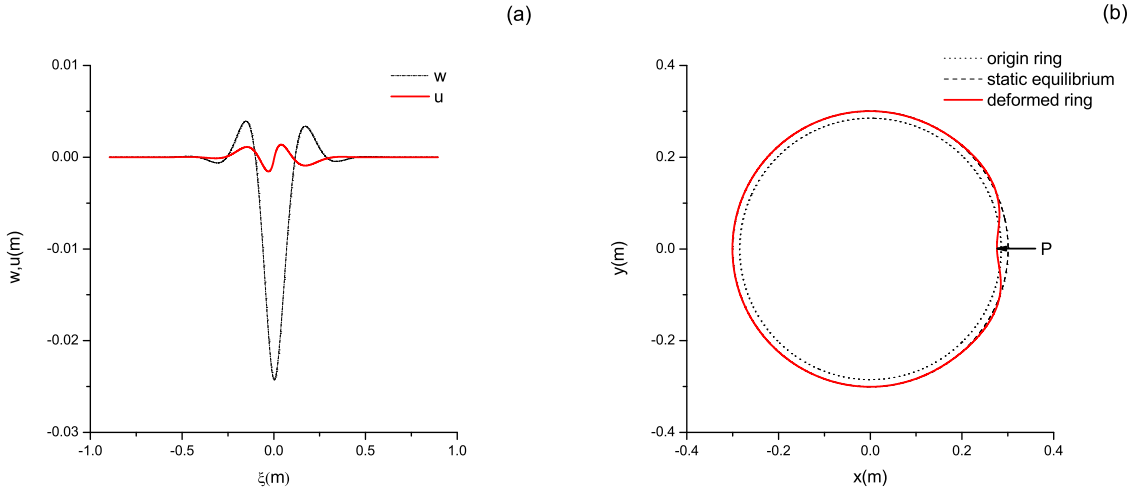

Figure 3: v=50m/s

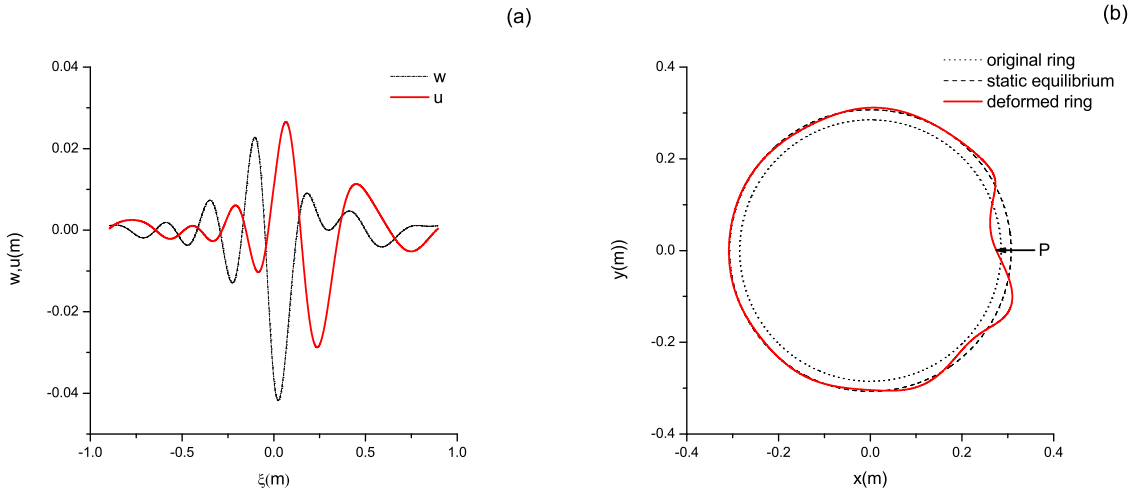

Figure 4: v=70m/s

the dotted line represents the original undeformed ring, the dash line represents the static equilibrium of the ring obtained by equation (4). The ring shape after deformation is depicted by solid line. Note that in all the figures, the ring rotates anticlockwise.

Three different velocities are considered. In Figure 3, the ring rotates with velocity $\nu = 50\mathrm{m/s}$, it is clearly seen that the ring deflections are symmetrical with respect to the loading point (the ring deflections are not perfectly symmetrical because of the damping, but if there is no damping or the rotating speed is small enough, the deflections will be perfectly symmetrical). In this case, it is obvious that the ring rotates at sub-critical speed. In Figure 4, the response for $\nu = 70\mathrm{m/s}$ is shown. Both the radial and the circumferential displacements become wave-like which indicates that the ring now is rotating at a velocity that is higher than the

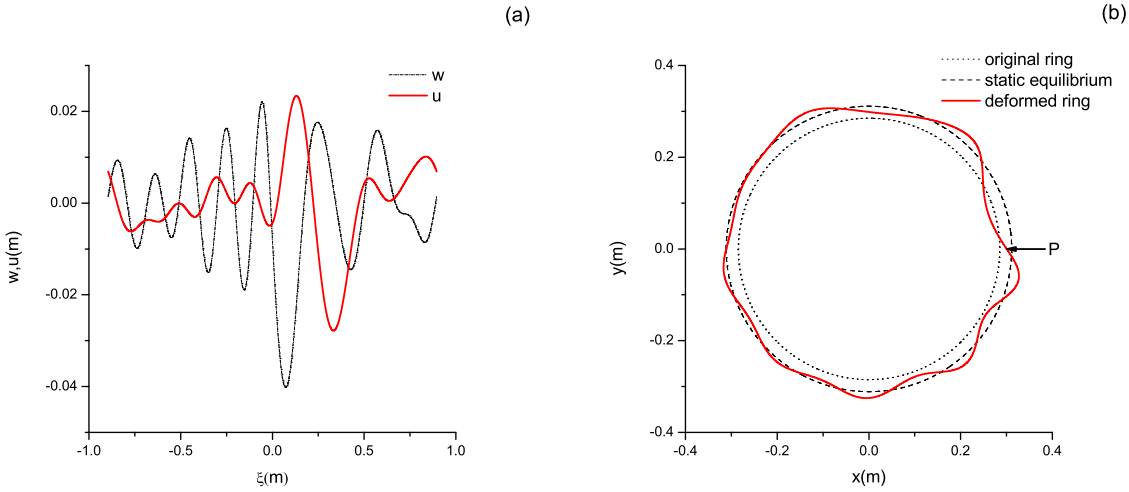

Figure 5: v=80m/s

critical speed. The displacements become more wavy and spread from the loading point to the whole ring in Figure 5 when the rotating speed increases to $v = 80\mathrm{m/s}$. Further calculation shows the critical speed to be about the same as the minimum phase speed $v = 62\mathrm{m/s}$ of a stationary ring with the same parameters.

6 Comments on other rotating ring models

In most publications, researchers claim that no critical speeds exist for rotating thin ring models, see for example Ref. [1]. As shown in this paper, when the model in Ref. [2] is chosen as a basis in our study, together with a modified pretension, steady state wave-like deformations are predicted. If one follows the procedure proposed in this paper and modifies the pretension to the form of equation (3), one may wonder if other rotating ring models are also capable of predicting the standing waves. Following the procedure presented in this paper, the other two popular rotating thin ring models proposed in Ref. [2, 3] are examined. The examinations show that they can predict critical speed as well, and the resulting critical speeds are similar to those obtained in Section 4 of this paper.

7 Conclusions

In this paper, the following conclusions are made:

Stationary modes for both bending dominant modes and extension dominant modes are reported for a rotating ring using the parameters of a pneumatic tire.

Critical speed is successfully predicted for a rotating ring.

The above formulated conclusions are based on one of the most popular rotating ring models with the modification of the pretension caused by rotation. Other rotating ring models may also be capable of predicting the existence of the critical speed provided that the same modification is implemented.

References

[1] S.C. Huang, W. Soedel, Response of rotating rings to harmonic and periodic loading and comparison with the inverted problem. Journal of Sound and Vibration, 118(2), 253-270, 1987.

[2] S. Gong, A study of in-plane dynamics of tires. PhD Thesis, Delft University of Tech-nology, 1993.

[3] Y.J. Kim, J.S. Bolton, Effects of rotation on the dynamics of a circular cylindrical shell with application to tire vibration. Journal of Sound and Vibration, 275(3), 605-621, 2004.

[4] A.V. Metrikine, M.V. Tochilin, Steady-state vibrations of an elastic ring under a moving load. Journal of Sound and Vibration, 232(3), 511-524, 2009..

[5] J. Padovan, On viscoelasticity and standing waves in tires. Tire Science and Technology, 4(4), 233-246, 1976.

[6] G.R. Potts, C.A. Bell, L.T. Charek, T.K. Roy, Tire vibrations. Tire Science and Tech-nology, 5(4), 202-225, 1977.

[7] S.C. Huang, B.S. Hsu, Resonant phenomena of a rotating cylindrical shell subjected to a harmonic moving load. Journal of Sound and Vibration, 136(2), 215-228, 1990.

[8] Y.T. Wei, L. Nasdala, H. Rothert, Analysis of forced transient response for rotating tires using REF methods. Journal of Sound and Vibration, 320(1), 145-162, 2009.

[9] L.H. Yam, D.H. Guan, A.Q. Zhang, Three-dimensional mode shapes of a tire using ex-perimental modal analysis. Experimental mechanics, 40(4), 369-375, 2000.

[10] T. Lu, A. Metrikine, A rotating ring in contact with a stationary load as a model for a flexible train wheel. EURODYN 2014: Proceedings of the 9th International Conference on Structural Dynamics, Porto, Portugal, 30 June-2 July 2014. Faculty of Engineering of University of Porto, 2014.

Tao Lu, Faculty of Civil Engineering and Geosciences, Delft University of Technology Stevinweg 1, 2628 CN Delft, The Netherlands

Andrei V. Metrikine, Faculty of Civil Engineering and Geosciences, Delft University of Technology Stevinweg 1, 2628 CN Delft, The Netherlands